Title: Homeostatic remodeling of mammalian membranes in response to dietary lipids is essential for cellular fitness

Short title: Homeostasis of mammalian membranes

Authors: Kandice R Levental*, Eric Malmberg, Yang-Yi Fan, Robert Chapkin, Robert Ernst, Ilya Levental*

Authors affiliations: Kandice R Levental[a], Eric Malmberg[a], Yang-Yi Fan[b], Robert Chapkin[b], Robert Ernst[c], Ilya Levental[a]

[a]University of Texas Health Science Center at Houston, Houston, TX, USA

[b]Program in Integrative Nutrition & Complex Diseases and Department of Nutrition & Food Science, Texas A&M University, College Station, TX, USA.

[c]Department of Medical Biochemistry and Molecular Biology, Medical Faculty, Saarland University, 66421 Homburg, Germany

***Co-corresponding authors:** Dr. Ilya Levental and Dr. Kandice Levental

Address: Suite 4.202A, 6431 Fannin St, Houston, TX, USA 77030

Phone: +1–713–500–5566

Fax: +1–713–500–7456

Email: ilya.levental@uth.tmc.edu ; kandice.r.levental@uth.tmc.edu

Keywords: membrane fluidity, lipidomics, diet, homeostasis, adaptation, saturated lipid, polyunsaturated fatty acid, cholesterol, SREBP

ABSTRACT

Biological membranes form the functional, dynamic interface that hosts a major fraction of all cellular bioactivity. Proper membrane physiology requires maintenance of a narrow range of physicochemical properties, which must be buffered from external perturbations. While homeostatic adaptation of membrane fluidity to temperature variation is a ubiquitous design feature of ectothermic organisms, such responsive membrane adaptation to external inputs has not been directly observed in mammals. Here, we report that challenging mammalian membrane homeostasis by dietary lipids leads to robust lipidomic remodeling to preserve membrane physical properties. Specifically, exogenous polyunsaturated fatty acids (PUFAs) are rapidly and extensively incorporated into membrane lipids, inducing a reduction in membrane packing. These effects are rapidly compensated both in culture and *in vivo* by lipidome-wide remodeling, most notably upregulation of saturated lipids and cholesterol. These lipidomic changes result in recovery of membrane packing. This lipidomic and biophysical compensation is centrally mediated by the sterol regulatory machinery, whose pharmacological or genetic abrogation results in decreased cellular fitness when membrane homeostasis is challenged by dietary lipids. These results reveal an essential mammalian mechanism for membrane homeostasis wherein lipidome remodeling in response to dietary lipid inputs preserves functional membrane phenotypes.

INTRODUCTION

Lipidic membranes are the essential barriers between life and the abiotic world and also mediate most intracellular compartmentalization in eukaryotic cells. However, the role of membranes is not limited to passive barriers. Approximately one third of all proteins are membrane-embedded [1], and many more are membrane-associated through post-translational modifications, lipid binding, and protein-protein interactions. Thus, a major fraction of cellular bioactivity occurs at membrane interfaces. Importantly, the physicochemical properties of the lipid matrix are key contributors to membrane physiology. A canonical example is membrane viscosity, which determines protein diffusivity, and thus protein-protein interaction frequency. Another is membrane permeability, which governs the diffusion of solutes into and out of the cytosol. Numerous other membrane physical parameters can determine protein behavior, including but not limited to fluidity, permeability, curvature, tension, packing, bilayer thickness, and lateral compartmentalization [2-12].

Because of their central role in protein function, effective maintenance of membrane properties is essential for survival in a complex and variable environment. In ectothermic (i.e. non-thermoregulating) organisms,

55 a pervasive challenge to membrane homeostasis comes in the form of temperature variations. Low
56 temperature reduces the motion of lipid acyl chains, causing membranes to laterally contract, stiffen, and
57 become more viscous [13]. Organisms across the tree of life, from prokaryotes to ectothermic animals,
58 respond to such perturbations by tuning membrane lipid composition, down-regulating tightly packing
59 lipids (e.g. containing saturated acyl chains) and up-regulating more loosely packed ones containing
60 unsaturations or methylations in their lipid tails [13-15]. This response was termed 'homeoviscous
61 adaptation', as these lipid changes result in remarkable constancy in membrane fluidity in spite of variable
62 growth conditions [13,14,16]. It is worth noting that while fluidity is maintained at a specific set point, it should
63 not be assumed that this is either the control variable, or the physical property being sensed; rather
64 membrane fluidity may correlate with other membrane/lipid control parameters. For example, membrane
65 homeostasis in *Bacillus subtilis* is mediated by the DesK sensor that is believed to sense membrane
66 thickness [17]. In the yeast endoplasmic reticulum (ER), recently discovered sensors are sensitive
67 specifically to lipid packing [5] and bilayer compressibility [18].

68 Excepting a few specialized instances (e.g. hibernation), mammals and other warm-blooded animals are
69 not subject to large-scale variations in body temperature; thus, there has been relatively little investigation
70 of homeostatic membrane responsiveness in such organisms. However, it is a well-established but under-
71 appreciated fact that mammalian membrane homeostasis is extensively challenged by dietary inputs.
72 Dietary lipids have major impacts on membrane compositions *in vivo* [19,20], and these perturbations must
73 presumably be buffered to maintain cellular functionality. Mammalian lipidomes are much more complex
74 [21-23] than either bacteria [24] or yeast [25,26], suggesting more potential control nodes required to balance the
75 various conflicting demands of mammalian membrane physiology.

76 The possibility of a homeoviscous response in mammalian cells was suggested by two studies in the 1970s,
77 which used a spontaneously arising mutant of Chinese Hamster Ovary (CHO) cells that is defective in
78 cholesterol regulation [27,28]. These mutants accumulate cholesterol compared to wild-type CHO cells, but
79 maintain normal membrane fluidity, possibly through modulation of their phospholipid profiles. However,
80 the molecular etiology of the defects in these mutants remains unknown, and it was not reported where
81 the cholesterol in these cells was accumulating (possibly storage organelles or lysosomes). Further,
82 limitations of then-available technologies prevented direct demonstration of lipidomic responses to
83 cholesterol modulation. Thus, the relevance of those insights to physiologically relevant perturbations of
84 metabolically normal mammalian cells remains unclear. More recently, homeoviscous adaptation in
85 mammals has been inferred from data-driven modeling approaches, which used the physical properties
86 (melting temperature, intrinsic curvature) of pure lipids to extrapolate those of complex, biological

87 membranes [29,30]. However, the inherent non-additivity [31] and non-ideality [32] of lipid mixtures suggests that
88 extrapolation of physical parameters of complex membranes from pure lipids may not be a reliable
89 approach. Finally, lipid composition and membrane properties have been implicated in the heat shock
90 response, though usually with a specific focus on signaling in the proteostasis network [33].

91 Here, we directly evaluate the hypothesis that mammalian membranes homeostatically adapt to dietary
92 inputs by characterizing the lipidomic and biophysical responses to dietary fatty acids in several
93 mammalian cell types and *in vivo*. We show that polyunsaturated fatty acids (PUFAs) are robustly
94 incorporated into membrane phospholipids, introducing significant biophysical perturbations. This
95 perturbation is counterbalanced by nearly concomitant lipidomic remodeling, most notable in the
96 upregulation of saturated lipids and cholesterol. This remodeling normalizes membrane biophysical
97 properties. These responses are centrally mediated by transcriptional sterol-regulatory machinery
98 involving the Sterol Regulatory Element Binding Protein SREBP2. Finally, we show that the homeostatic
99 membrane response is essential for cellular fitness, as abrogation of key response nodes leads to cytotoxic
100 effects when membrane homeostasis is challenged by exogenous fatty acids.

101

102 **RESULTS**

103 *Robust and specific incorporation of PUFAs into membrane lipids*

104 Recent observations revealed that supplementation of cultured mammalian mast cells (rat basophilic
105 leukemia cells (RBL)) with docosahexaenoic acid (DHA) leads to robust incorporation of this dietary
106 polyunsaturated fatty acid into membrane lipids [23]. We observed similar effects in isolated human
107 mesenchymal stem cells [34], cultured Chinese hamster ovary (CHO) cells, and rat primary hippocampal
108 neurons (Supp Fig S1), confirming that uptake and incorporation of exogenous DHA into membrane lipids
109 is not cell-type specific. Supplementation designed to recapitulate DHA-enriched diets in mammals (see
110 Materials and Methods) increased the fraction of DHA-containing glycerophospholipids (GPLs) by nearly
111 15-fold (from <1 to ~15 mol%) (Fig 1A). Similarly, supplementation with the more common PUFA ω-6
112 arachidonic acid (AA) increased the fraction of AA-containing lipids by >3-fold (Fig 1B). Surprisingly,
113 supplementation with monounsaturated (oleic; OA) acid or saturated (palmitic; PA) fatty acid produced
114 only minimal lipidomic changes (Supp Fig S2). We speculate that this disparity in incorporation between
115 PUFAs and more saturated FAs is associated with their availability in cell culture media: cells have access
116 to sufficient levels of OA and PA such that supplementation has no effect, whereas PUFA levels are

117 limited such that supplementation with the physiologically appropriate concentrations used here leads to
118 robust uptake and incorporation.

119 To confirm that the membrane incorporation of supplemented PUFAs in cultured cells appropriately
120 recapitulates *in vivo* conditions, we analyzed the membrane lipidomes of mouse hearts and livers after two
121 weeks of free-feeding on chow containing either fish oil (FO; 22.5% w-3 PUFAs, detailed fatty acid
122 composition in Supplement) or corn oil (CO; 1.3% w-3 PUFAs), as previously described[35]. Consistent
123 with previous observations[35-37] and the *in vitro* measurements here, dietary fish oil supplementation
124 produced a robust incorporation of DHA into membrane lipids, with ~3-fold and ~30-fold more DHA-
125 containing membrane lipids in the FO-fed versus CO-fed livers and hearts, respectively (Fig 1D-E).
126 Interestingly, this effect was not observed for storage lipids (i.e. triglycerides, TAGs), as DHA did not
127 incorporate into TAGs to a notable extent (not shown).

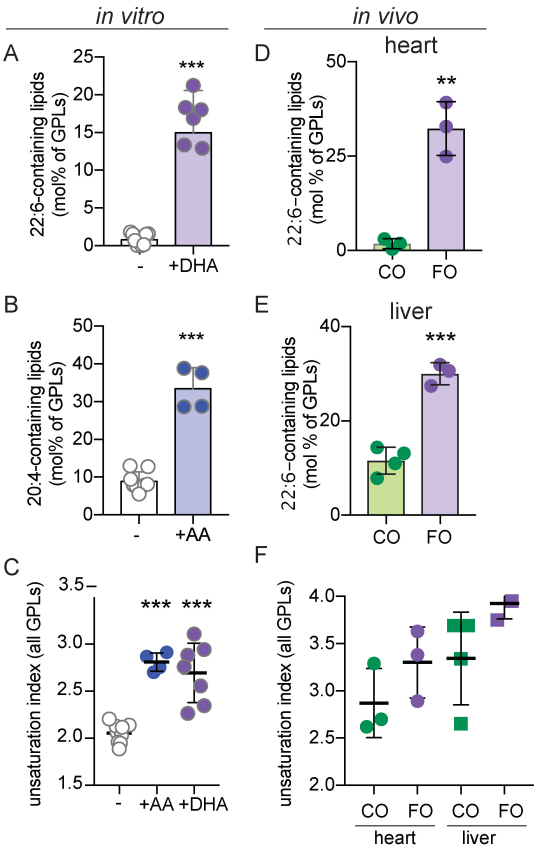

128

129 **Fig 1. Supplemented PUFAs are robustly and specifically incorporated into membrane phospholipids *in vitro* and *in***
130 ***vivo*.** Supplementation of culture media with (A) DHA or (B) AA for 3 days (20 μM) leads to dramatic increase in levels of PUFA-
131 containing membrane lipids in RBL cells, which (C) results in a significant increase in the overall unsaturation of membrane
132 lipids. The unsaturation index is a concentration-weighted average lipid unsaturation. Mice fed diet rich in fish oil (FO) have
133 significantly increased lipids containing DHA in the (D) hearts and (E) livers compared to corn oil (CO) fed. (F) Incorporation of

134 dietary FAs results in increase in the overall unsaturation of membrane glycerophospholipids (F). Individual experiments (A-C)
135 or animals (D-F) are shown. Bars represent mean ± SD. **p<0.01, ***p<0.001 for student's t-test compared to untreated.
136 Treatment with saturated (PA) or monounsaturated (OA) fatty acids in these conditions had no effect on the lipidome (see Fig
137 S2).

138

139 *Lipidome remodeling associated with PUFA incorporation*

140 Despite the copious incorporation of exogenous PUFAs into membrane lipids and the resulting increase
141 in overall membrane unsaturation (Fig 1), cells *in vitro* did not show any obvious toxicity or differences
142 in proliferation. This observation was somewhat surprising in light of the central role of lipid unsaturation
143 in membrane physical properties [38,39] and the critical role of those properties in regulating various cellular
144 processes [3,4,7]. Thus, we hypothesized that mammalian cells may compensate for perturbations from
145 exogenous FAs by remodeling their lipidomes. Indeed, while treatments with OA/PA had no effect on
146 overall cell lipidomes (Supp Fig S2; consistent with their lack of incorporation), both AA and DHA
147 supplementation reduced the abundance of other polyunsaturated (i.e. di- and tri-unsaturated) lipid species
148 (Fig 2A-B). This effect could potentially be explained by replacement of these PUFA-containing lipids
149 by AA/DHA-containing ones. Much more surprising was the highly significant increase in fully saturated
150 lipids resulting from PUFA supplementation, due to significantly increased abundance of phospholipid-
151 incorporated saturated fatty acids (Fig 2A-B). We note that for accurate estimates of lipidomic remodeling
152 the supplemented FAs are removed from the analysis (e.g. ω-3-containing lipids from DHA-supplemented
153 data), as the rather extreme over-abundance of those species upon supplementation suppresses the
154 visualization of compensatory effects (original data are shown in Fig S3A). This analysis reveals
155 approximately 2-fold and 4-fold more fully saturated lipids resulting from DHA and AA supplementation,
156 respectively (Fig 2A-B). These changes were associated with significantly reduced overall unsaturation
157 in phospholipids not containing the supplemented FAs (Fig 2A-B, insets). These effects were, at least in
158 part, transcriptionally mediated, as evidenced by mRNA levels of the major fatty acid desaturase enzymes
159 SCD1 and SCD2. As previously reported [40], both were substantially down-regulated by DHA treatment
160 (Fig S4), consistent with more saturated and fewer polyunsaturated lipids. Similar compensatory effects
161 were observed for lipid length. Both AA (20-carbon) and DHA (22-carbon) are relatively long FAs, and
162 thus their incorporation increased the overall length of membrane phospholipids (Fig S3B-C). However,
163 there was also a notable increase in relatively short non-DHA/AA containing lipids (Fig S3D-E). The
164 headgroup profile of membrane lipids was not notably affected by any of the treatments (Supp Fig S3F).

165 This lipidomic remodeling in response to PUFA feeding *in vitro* was not limited to a single cell type. The
166 observations described so far were on a transformed leukocyte cell line (RBL); however, very similar
167 DHA-induced lipid changes were observed in cultured CHO cells, primary rat hippocampal neurons,
168 primary human MSCs, and MSCs that were differentiated *in vitro* into osteoblasts or adipocytes (Fig. 2C).
169 Remarkably, not only the broad trends of the lipidomic remodeling (more saturated, less unsaturated
170 lipids) were common between these disparate cell lineages and sources, but also the magnitude of the
171 effects were quantitatively similar, despite drastic differences in overall lipid composition [23,34,41,42]. The
172 similarity of the responses between freshly isolated cells, cultured primary cells, and long-term cultured
173 cells lines derived from two different germ layers and three different organisms suggests that
174 comprehensive lipidomic remodeling in response to exogenous PUFAs is a general phenomenon for
175 mammalian cells.

176 Importantly, we confirmed that this response also occurs *in vivo*. The incorporation of dietary ω-3 PUFAs
177 into mouse heart membrane lipids led to remarkably similar lipidomic remodeling as was observed in
178 cultured cells. Namely, we observed ~3-fold increase in saturated lipids and 50% increased levels of
179 monounsaturated lipids (Fig 2D). Concomitantly, there was a notable reduction in polyunsaturated lipids
180 not containing ω-3 PUFAs. Altogether, the non-ω-3 PUFA lipids were significantly more saturated in
181 heart membranes from FO-fed animals (Fig 2D, inset), fully consistent with compensatory, homeostatic
182 lipidomic remodeling *in vivo*.

183

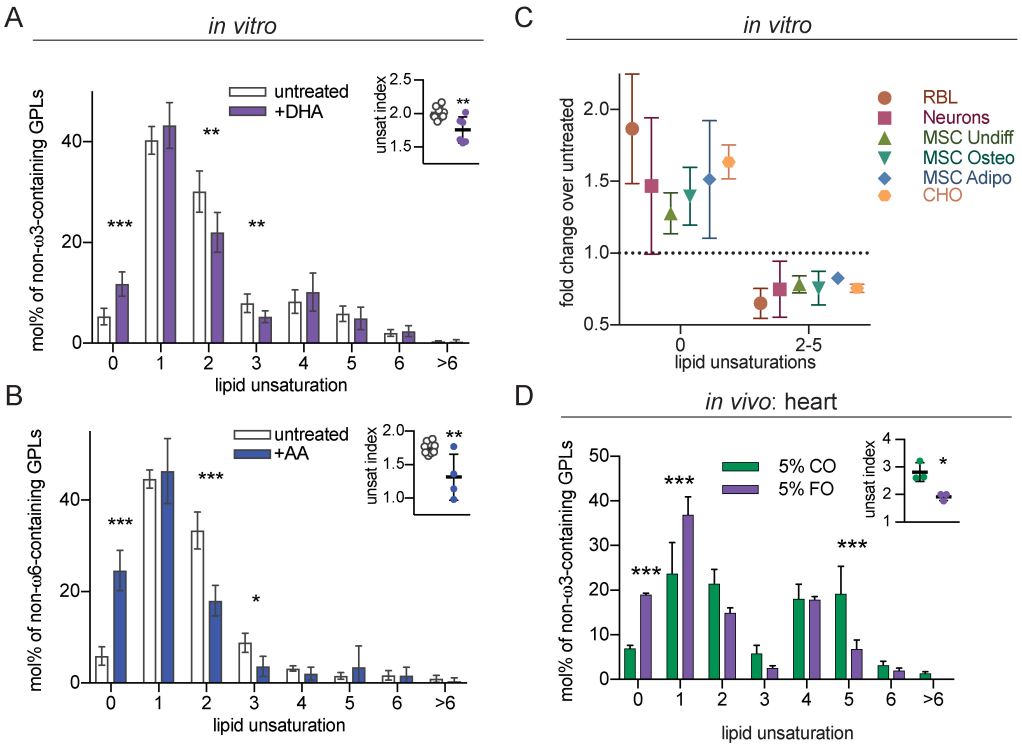

Figure 2 – Lipidome remodeling induced by PUFA supplementation. Lipidome-wide remodeling of lipid unsaturation induced by (A) DHA or (B) AA supplementation. Both PUFAs induce significant upregulation of saturated lipids and downregulation of lipids containing di- and tri-unsaturated lipids. Data shown are for membrane phospholipids not containing the supplemented lipid, i.e. DHA-containing lipids in (A) and AA-containing in (B). Raw lipidomes in Fig S3A show the same trends. (insets) Unsaturation index (concentration-weighted average lipid unsaturation) of non-DHA/AA-containing lipids is significantly reduced upon PUFA supplementation. (C) DHA-mediated lipidomic remodeling, indicated by increased saturated lipids and decreased polyunsaturated lipids (2-5 unsaturations), is consistent across multiple cell types, including isolated rat hippocampal neurons, cultured human MSCs, and MSC differentiated into adipogenic or osteogenic lineages. (D) Lipid unsaturation profiles in membrane lipids isolated from murine heart tissue after feeding with CO versus FO. Incorporation of ω-3 PUFAs into membrane lipids (see Fig 1D) induced robust lipidomic remodeling, increasing saturated and monounsaturated lipids, reducing other PUFA-containing lipids, thereby (inset) decreasing overall unsaturation. All data shown are average +/- SD for n ≥ 3 biological replicates. A, B, and D are two-way ANOVA with Sidak's multiple comparison test. Insets are student's t-test compared to untreated. *p<0.05, **p<0.01, ***p<0.001.

Lipidomic remodeling is nearly concomitant with exogenous PUFA incorporation

The remodeling associated with PUFA incorporation into membrane lipids suggested the induction of a homeostatic membrane response, wherein saturated lipids are upregulated to compensate for the fluidizing effect of PUFA-containing species. To support this inference, we analyzed the temporal profiles of PUFA incorporation and associated lipidomic changes *in vitro*. DHA was rapidly incorporated into membrane lipids, with significant increases in DHA-containing lipids observed within 1 h of supplementation and

205 half-time of incorporation of ~4 h (Fig 3A-B). The recovery time course was significantly slower, as wash-
206 out of DHA was followed by a return to baseline with a half-time of ~25 h (Fig 3C). This is the
207 approximate doubling time of RBL cells in culture, suggesting that the "wash-out" effect likely results
208 from dilution by new lipid synthesis rather than directed removal of DHA from membrane lipids.
209 Remarkably, the associated lipidome remodeling proceeded with nearly identical temporal profiles to both
210 DHA supplementation and wash-out (Fig 3D-I). The increase in saturated lipids (Fig 3E) and the decrease
211 in di-unsaturated lipids (Fig 3H) were essentially concomitant with DHA incorporation and similar time
212 courses were also observed for the wash-out (Fig 3F and 3I). These observations reveal unexpectedly
213 rapid lipidomic changes to membrane lipid perturbations and suggest that such perturbations induce nearly
214 simultaneous compensatory responses.

215 The nature of the broad compensatory lipidomic remodeling in response to PUFA supplementation in
216 mammalian cells evokes classical observations of homeoviscous adaptation in ectothermic (e.g. non-
217 thermoregulating) organisms [13-16]. There, perturbations of membrane physical properties produced by
218 changes in ambient temperature are rapidly compensated by lipidomic changes apparently designed to re-
219 normalize membrane physical properties. Our findings suggest that a similar response to fluidizing stimuli
220 occurs in mammalian cells, where it has been co-opted to cope with perturbations from exogenous lipids
221 (e.g. from the diet).

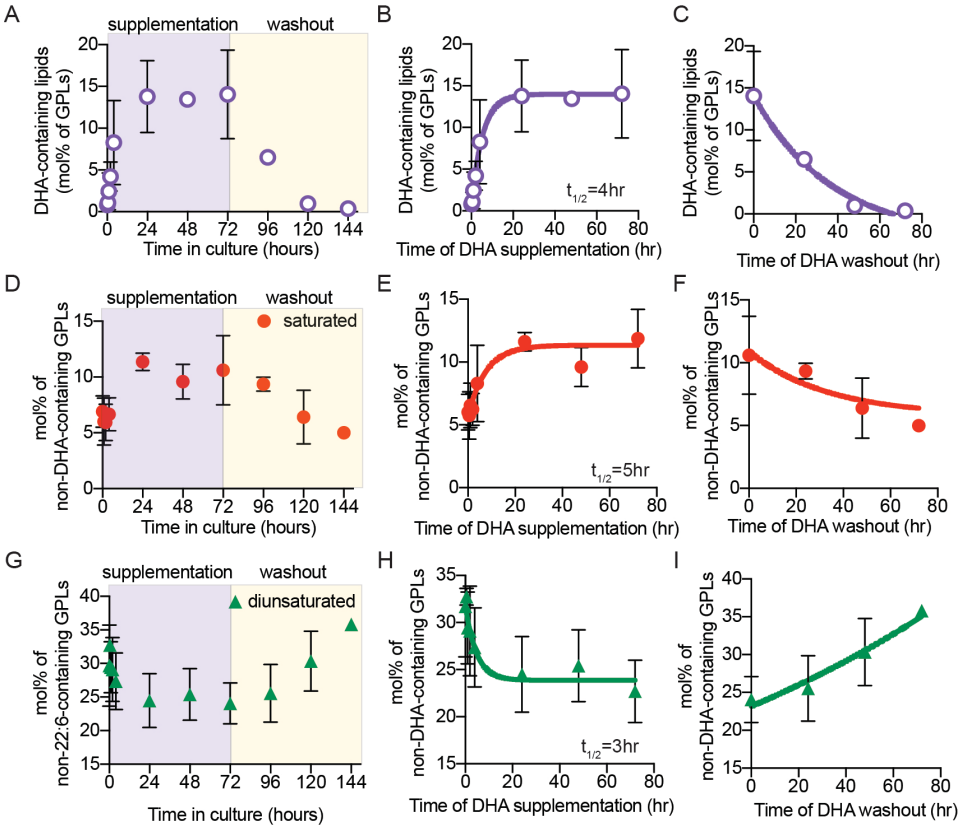

Figure 3 – Time course of DHA incorporation and lipidome remodeling. (A-C) Time course of DHA incorporation into GPLs following supplementation, then wash-out. Time course of concomitant (D-F) saturated lipid and (G-I) di-unsaturated lipid changes induced by DHA supplementation. All data shown are average +/- SD for n ≥ 3 biological replicates.

Cholesterol upregulation by DHA via SREBP2

The above-described acyl chain remodeling in response to PUFA supplementation was incomplete, as the unsaturation index of PUFA-supplemented cells remained higher than those from untreated controls (Fig 1C and 1F). If this lipidome response were designed to normalize membrane properties, the acyl chain remodeling appears insufficient on its own, and there was no remodeling of GPL headgroups. In contrast to most prokaryotes where membrane homeostasis is mediated largely by glycerolipids [14], membrane properties in more complex organisms are regulated to a very significant extent by sterols [43,44]. Thus, we hypothesized that the adaptive response to PUFA perturbation in mammalian cells is also mediated by cholesterol. Indeed, DHA supplementation significantly increased membrane cholesterol over the un-supplemented baseline in both murine heart tissue (Fig 4A) and cultured cells (Fig 4B). In cells, the increase in cholesterol abundance was again quite rapid, with effects observed within 1 h of DHA introduction and reaching a peak after ~4 h (Fig 4C), essentially concomitant with the acyl chain

239 remodeling (Fig 3). There was also evidence of a small but notable overshoot, as the cholesterol increase
240 was somewhat attenuated after ~4 hrs. These observations suggest that cholesterol upregulation is an early
241 and potent response to membrane perturbation.

242 The machinery for cholesterol production in metazoans is regulated by proteolytic processing of
243 transcription factors of the sterol regulatory element binding protein (SREBP) family [45]. Specifically,
244 signals to upregulate cellular cholesterol levels are translated into proteolysis of a membrane-bound
245 SREBP2 precursor to release a 'mature' cleaved fragment, which translocates to the nucleus to induce
246 transcription of various target genes, including those for cholesterol synthesis and uptake [45]. Having
247 observed a robust and rapid increase in cholesterol levels resulting from DHA supplementation, we
248 evaluated whether SREBP2 processing was associated with this response. Indeed, DHA feeding increased
249 the production of the 'mature' transcription factor form of SREBP2, with minimal effect on the precursor
250 form (Fig 4D).

251 These findings suggested that processing of SREBP2 is involved in homeostatic membrane remodeling
252 of mammalian lipid composition in response to perturbation by PUFA incorporation. To test this
253 inference, we measured the response to PUFA supplementation in cells where SREBP processing was
254 inhibited either genetically or pharmacologically. SRD-12B cells are clonal variants of CHO cells wherein
255 a genetic defect in the Site 1 Protease (S1P; cleaves SREBPs to produce the transcriptionally active forms)
256 prevents SREBP processing/activation [46]. In these cells, no notable upregulation of cholesterol (Fig 4E)
257 or saturated lipids (Fig S5) was observed upon DHA supplementation. Similarly, chemical inhibition of
258 SREBP processing by the pentacyclic triterpene betulin [47] completely abrogated DHA-induced
259 upregulation of cholesterol (Fig 4B, triangles) and saturated lipids (Fig S6). These results support the
260 crucial role for SREBP2 in lipidomic remodeling induced by PUFAs.

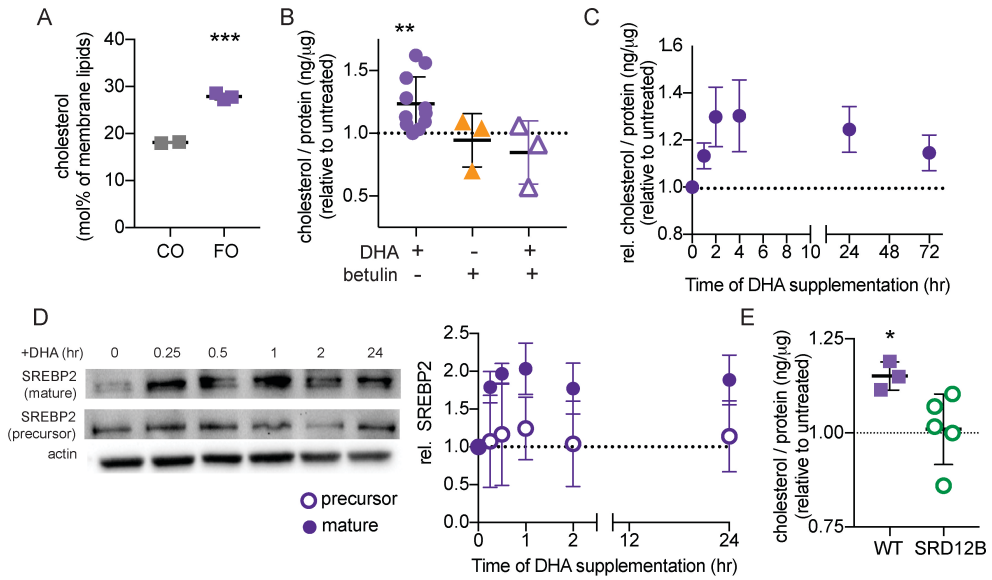

Fig 4 – Cholesterol upregulation by DHA supplementation. (A) Cholesterol is increased in membrane lipids isolated from murine heart tissue after feeding with FO as compared to CO. (B) Membrane cholesterol is significantly increased by DHA supplementation. Cells treated with 200 nM betulin did not upregulate cholesterol upon DHA supplementation. (C) Time course suggests cholesterol increase is a rapid response to DHA-mediated membrane perturbation. (D) The 'mature', transcription-competent form of SREBP2 is rapidly produced in response to DHA supplementation. (E) Cholesterol is significantly increased in WT CHO cells treated with DHA; this effect is abrogated in cells with a defect in SREBP activation (SRD12B; S1P-negative). All data shown are average +/- SD for n ≥ 3 biological replicates; ***p<0.001 in (A) is one-sample t-test between groups; *p<0.05, **p<0.01 in B and E are one-sample t-tests compared to untreated.

Physical homeostasis following lipidomic perturbation

The above data reveal rapid and comprehensive lipidomic remodeling resulting from the incorporation of DHA into membrane lipids, wherein lipids that decrease membrane fluidity / increase membrane packing (saturated lipids and cholesterol) are rapidly upregulated in response to introduction of PUFA-containing lipids that increase membrane fluidity. These changes are consistent with lipidome remodeling for the purpose of homeostatic maintenance of membrane physical properties. To directly evaluate this inference, we measured membrane packing in live cells using a fluorescence assay that relies on a solvatochromic dye (C-Laurdan) whose spectral characteristics are dependent on membrane properties [48]. Specifically, the emission spectrum of C-Laurdan is red-shifted in loosely-packed membranes (due to the enhanced polarity of the fluorophore nano-environment), and the relative extent of this spectral shift can be quantified by ratiometric spectroscopy or imaging [49]. The resulting dimensionless parameter called

282 Generalized Polarization (GP) is a widely used proxy for membrane packing and fluidity [50-54], with higher
283 values reporting more tightly packed membranes.

284 Fig 5A shows a map of C-Laurdan GP in live cells generated by confocal spectral imaging [55]. The
285 relatively fluid (low GP; blue/green pixels) internal membranes and relatively packed plasma membranes
286 (high GP; yellow/red pixels) are characteristic of mammalian cells [49,51] (see trace right). These clearly
287 distinct regions enabled us to separately quantify the effects of DHA on plasma versus internal membranes
288 (Fig 5B). The packing of internal membranes was significantly decreased shortly after introduction of
289 exogenous DHA (purple circles; pooled data for 2 and 4 h time points are different from 0 with $p < 0.01$),
290 suggesting reduced packing consistent with the known fluidizing effect of PUFA-containing lipids [23,56].
291 This response eventually reversed, with GP fully normalizing to baseline by 24 h. Thus, DHA
292 incorporation combined with the associated remodeling produced no net change in overall membrane
293 properties. This renormalization of membrane packing was markedly reduced when lipidomic remodeling
294 was inhibited by targeting SREBP processing. Namely, betulin treatment suppressed the recovery of
295 membrane packing following DHA treatment (Fig. 5B, orange symbols and line), leading to significantly
296 reduced GP in DHA-treated RBL cells after 24 h (Fig. 5B-C). Similarly, while wild-type CHO cells did
297 not show a significant effect of DHA on membrane fluidity after 24 h treatment, DHA supplementation
298 of SRD-12B cells exhibited significantly reduced GP.

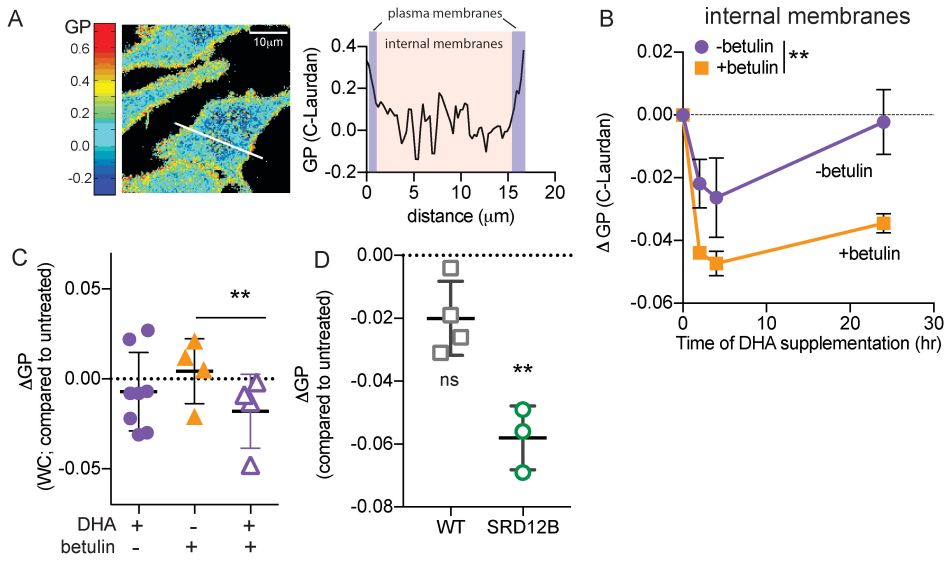

299

300 **Fig 5 – Physical membrane homeostasis.** (A) Exemplary GP map of RBL cells showing the characteristically tighter lipid
301 packing (i.e. greater GP) of the PM compared to internal membranes. (right) line scan of GP across a single cell shown by the
302 white line in the image. (B) Temporal changes in lipid packing (GP) after DHA supplementation and betulin treatment. In control
303 cells, internal membranes initially fluidized by excess DHA-containing lipids (purple) recovered to baseline by 24 hrs. In contrast,

304 internal membrane packing did not recover in betulin-treated cells (orange). Effect of treatment was significant (p<0.01) by 2-
305 way ANOVA; each time point for betulin-treated cells was significantly different from zero (p<0.01). (C) Neither DHA or betulin
306 affected membrane packing (GP) alone, whereas cells treated with DHA in the presence of betulin had significantly reduced
307 membrane packing. (D) DHA supplementation of WT CHO cells resulted in no change in membrane packing after 24 h, whereas
308 SRD-12B cells (defective in SREBP processing) had significantly reduced membrane packing. Average +/- SD for n ≥ 3 biological
309 replicates. ΔGP represent GP of treated cells normalized to untreated cells within each individual experiment. **p<0.01 in (C-
310 D) is for one-sample t-tests between groups. **p<0.05 in (B) is significance for effect of betulin treatment in 2-way ANOVA.

311

312 *Disruption of membrane homeostasis reduces cell fitness*

313 In unicellular organisms, the homeoviscous lipidomic response is necessary for maintaining membrane
314 physical properties in a range compatible with the biochemical processes necessary for life [13,15]. Having
315 observed similar lipidomic and biophysical responses in mammalian membranes, we hypothesized that
316 this adaptation was necessary for cellular fitness under conditions of membrane stress. To test this
317 hypothesis, we evaluated the cytological effects of DHA under chemical or pharmacological inhibition of
318 key homeostatic response nodes. Neither DHA nor betulin alone showed significant cytostatic effects;
319 however, DHA supplementation in the presence of betulin led to ~50% decrease in cell number after 3
320 days of culture (Fig 6A; full dose-response in Supp Fig S7). Similar effects were observed by inhibiting
321 fatty acid synthase (via 10 nM GSK2194069; Fig 6B), which is presumably necessary for production of
322 fatty acids towards the phospholipid remodeling described in Figures 2-3. These observations were
323 confirmed in SRD-12B cells, whose genetic lesion renders them incapable of activating SREBP [46] and
324 mounting an adaptive lipidomic and biophysical response to DHA supplementation (Figs 4E and 5D).
325 Consistent with the abrogated homeostatic response, DHA had a significant cytostatic effect on SRD-12B
326 cells (Fig 6C, green). These results reveal that inhibition of lipidome remodeling in mammalian cells
327 markedly reduced cellular fitness upon membrane perturbation with dietary fatty acids.

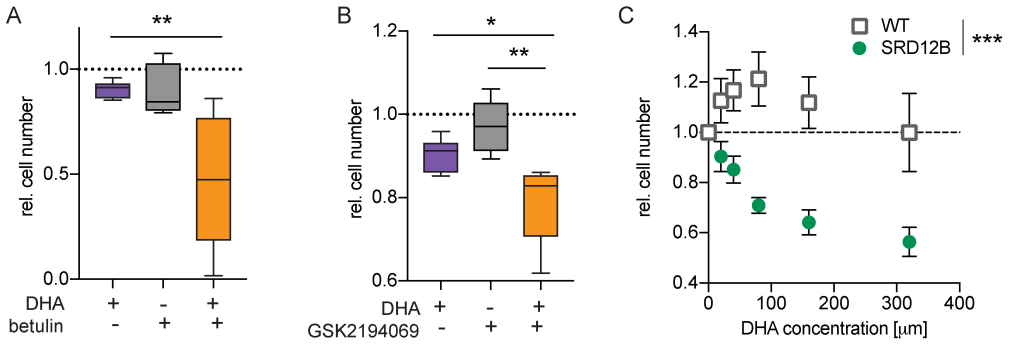

328

329 **Fig 6 – Inhibition of homeostatic lipidome remodeling reduces cell fitness under DHA supplementation.** (A) 200nM
330 betulin completely abrogated DHA-induced upregulation of cholesterol and (B) saturated lipids. (C) Neither DHA nor betulin

alone had a significant effect on cell numbers, whereas the combination was significantly cytostatic. (B) A similar synergistic effect was observed with DHA and GSK2194069 (FAS inhibitor; 10 nM). (C) In SRD-12B cells, which fail to upregulate cholesterol and saturated lipids upon DHA treatment (see Fig 4D and Supp Fig S6), DHA significantly inhibited cell growth, in contrast to control WT CHO cells, wherein DHA showed a slightly mitogenic effect. All data shown as average +/- SD for ≥ 3 independent experiments. A-B are student's t-tests; C is two-way ANOVA for effect of treatment. *p<0.05, **p<0.01, ***p<0.001.

DISCUSSION

The incorporation of dietary fatty acids into mammalian membrane lipids has been widely observed both *in vitro* [23,57,58] and *in vivo* [19,20,36,37,59]. The fact that exogenous fatty acids are so readily used for lipid synthesis is unsurprising in light of the fact that the enzyme required for *de novo* fatty acid production (fatty acid synthase) is minimally expressed in most adult human tissues [60]. Indeed, *de novo* lipogenesis is considered "negligible" [61,62] in adult humans, suggesting that exogenous sources of fatty acids are the major raw material for maintenance and replenishment of membrane lipids. This reliance on exogenous inputs for production of components central to cellular architecture and function would seem to present a major complication for homeostasis.

In ectothermic organisms, homeostatic membrane control has been widely observed in the form of homeoviscous adaptation [13-15]. According to this hypothesis, the relative abundance of saturated to unsaturated membrane lipids is responsive to temperatures changes in order to maintain membrane fluidity at the level required for the many processes hosted and regulated by cell membranes. Although such adaptation has been proposed in prokaryotes [14], single-celled eukaryotes [63], and even cold-blooded animals [64,65], studies on endothermic organisms have been limited [28,29], and there has yet been no direct observations of HVA in mammals or isolated mammalian cells. Our data directly confirm the three major tenets of cell-autonomous homeoviscous adaptation: (1) lipidomic remodeling resulting from a perturbation of membrane physical properties (Fig 2-4); (2) recovery of baseline physical properties at a new lipid composition (Fig 5); and (3) necessity of this response for cellular fitness (Fig 6). These observations suggest that mammalian cells possess the capacity for homeostatic membrane adaptation analogous to HVA, and that this response can compensate for perturbations from dietary lipid inputs.

In cold-blooded animals, the homeostatic membrane response also involves modulation of cholesterol levels [44,65], and we observe a similar response in mammalian cells, mediated at least partially through activation of SREBP2 (Fig 4). It is quite remarkable to note that disruption of SREBP activation either by betulin or in SRD-12B cells resulted in near-complete abrogation of the compensatory response. This abrogation was notable not only in the lack of cholesterol upregulation (Fig 4D and 6A), which may have

363 been expected, but also in the failure to upregulate saturated lipids (Figs S5 and S6), a response not directly
364 connected to SREBP2 target genes.

365 Our implication of SREBP2 as a critical node of the sense-and-respond module for membrane adaptation
366 is consistent with the central role of SREBPs in membrane homeostasis [45]. SREBP transcription factors
367 have been dubbed the "master regulators of lipid homeostasis", because they direct not only cholesterol
368 synthesis and uptake, but also proteins associated with membrane lipid metabolism, including those
369 involved in FA synthesis, elongation, and desaturation [66]. The effect of PUFA supplementation on SREBP
370 function has been extensively studied, and DHA is known to suppress the activation of SREBP1 and its
371 target genes, both in cultured cells and *in vivo* [67-69]. We observed downregulation of two SREBP1 target
372 genes (SCD1 and SCD2, Fig S3) suggesting a similar effect in our cells. In contrast, SREBP2 is not
373 suppressed by PUFAs [67,68], revealing that these two complementary regulators of membrane homeostasis
374 have different functions, despite both being sensitive to membrane cholesterol. In our observations,
375 SREBP2 is induced as a necessary part of the homeostatic response. Previous reports [68] have not noted a
376 significant effect of PUFAs on SREBP2, possibly because those experiments involved acute PUFA
377 feeding of serum-starved cells, where high levels of activated SREBPs may have suppressed the DHA-
378 mediated stimulation we observe here. We have confirmed this effect in our cells (not shown). It remains
379 to be determined whether SREBP2 is simply an effector of membrane remodeling downstream of yet-
380 unidentified sensing machinery, or whether this protein (and/or its regulatory machinery) may itself be
381 capable of sensing perturbations in membrane physical properties. Direct demonstration of protein
382 responsiveness to membrane packing has recently been described for two yeast ER proteins [5,18], providing
383 a conceptual and methodological toolbox for identifying other membrane sensors. Remarkably, despite
384 the ubiquity and importance of membrane homeostasis, the machinery used for sensing membrane
385 properties remains largely uncharacterized. It is an intriguing observation that Ire1, a core component of
386 the unfolded protein response (UPR), exhibits a dual sensitivity to unfolded proteins and aberrant lipid
387 compositions, demonstrating a tight connection between protein-folding and membrane properties [18]. This
388 connection suggests that the machinery for ameliorating protein-folding stresses may also be involved in
389 transducing and mitigating membrane stress [70].

390 In summary, our observations strongly support the hypothesis that mammalian cells in culture and *in vivo*
391 sense membrane physical properties and respond to perturbations by comprehensive remodeling of their
392 lipidomes. In our measurements, the perturbations were induced by supplementation with polyunsaturated
393 fatty acids (PUFAs); however, it is likely that other fats (e.g. cholesterol) or amphiphiles (bile acids,
394 anesthetics) may induce similar responses. We implicate SREBP2 as a central response mediator and show

395 that the compensatory response is important for cell fitness, confirming membrane adaptation as a central
396 requirement for cellular homeostasis.
397

398 **MATERIALS AND METHODS**

399 ***Materials:*** Betulin and GSK2194069 were obtained from Sigma Aldrich. C-Laurdan was purchased from
400 TPProbes (South Korea). Amplex Red kit to quantify cholesterol was purchased from Invitrogen.
401 Antibodies used: actin (monoclonal clone AC-15, Abcam), SREBP2 (polyclonal, Abcam).

402 ***Cell culture:*** Rat basophilic leukemia (RBL) cells were maintained in medium containing 60% modified
403 Eagle's medium (MEM), 30% RPMI, 10% fetal calf serum, 100 units/mL penicillin, and 100 μg/mL
404 streptomycin. Chinese hamster ovary (CHO) cells were maintained in DMEM:F12 (1:1) containing 5%
405 fetal calf serum, 100 units/mL penicillin, and 100 μg/mL streptomycin. SRD12B cells were maintained
406 in DMEM:F12 (1:1) containing 5% fetal calf serum, 50μM sodium mevalonate, 20μM oleic acid, 5μg/mL
407 cholesterol, 100 units/mL penicillin, and 100 μg/mL streptomycin. All cells were grown at 37ºC in
408 humidified 5% CO2.

409 ***Fatty acid treatments:*** Fatty acid stock solutions were received as air-purged ampules (Sigma Aldrich)
410 and loaded into BSA immediately upon opening. BSA loading was accompanied by stirring the fatty acid
411 with BSA dissolved in water (2:1 mol/mol FA:BSA), sterile filtering, purging with nitrogen prior to
412 aliquoting, and storing at -80°C. BSA loading, purging, and cold storage were all done to minimize FA
413 oxidation. For all experiments with FA supplementation, cells were incubated with 20 μM FA for 3 days
414 (cells were re-supplemented 24 h prior to analysis). Serum-containing, rather than serum-free, media was
415 used to approximate physiological supplementation, rather than exclusive introduction of specific FAs.
416 These conditions were chosen to approximate *in vivo* settings produced by DHA-enriched diets in
417 mammals: plasma free FA concentrations range from 300 to 750 μM [59,71] and up to 10 mol % of plasma
418 fatty acids are ω-3 DHA in rats fed a high-fish-oil diet [59]. Further, diets rich in ω-3 PUFAs led to
419 significant incorporation of these fats into cell membrane lipids [19,37,59], similar to the levels we observed
420 under our culture feeding conditions (Fig. 1). For these reasons, we believe our culture conditions
421 reasonably approximate physiological dietary membrane perturbations.

422 ***Animals and diets:*** All experimental procedures using laboratory animals were approved by the
423 University Laboratory Animal Care Committee of Texas A&M University. Pathogen-free female
424 C57BL/6 mice (n=180; Frederick Research Facility, Frederick, MD) weighing 16–18 g, were randomly

425 divided into two groups of 90. For 2 wk, mice had free access to one of the two semipurified diets, which
426 were adequate in all nutrients [35]. Diets varied only in the oil composition, i.e., either corn oil (CO) or an
427 (n-3) PUFA-enriched fish-corn oil (FO) mixture (4:1, w/w) at 5 g/100 g diet. The basic diet composition,
428 expressed as g/100 g was: casein, 20; sucrose, 42; cornstarch, 22; cellulose, 6; AIN-76 mineral mix, 3.5;
429 AIN-76 vitamin mix, 1, DL-methionine, 0.3; choline chloride, 0.2; Tenox 20A (containing 32% glycerol,
430 30% corn oil, 20% tert-butylhydroquinone, 15% propylene glycol, 3% citric acid) 0.1; and oil, 5. The fatty
431 acid composition of the diets, as determined by gas chromatography, is shown in Supplemental Table 1.
432 Mice were killed by CO2 asphyxiation after two weeks of feeding the CO/FO diet, and the livers and
433 hearts were isolated and frozen in liquid nitrogen. 20-50 mg of tissue was mechanically homogenized in
434 Dulbecco's PBS (without Ca^{2+} and Mg^{2+}). Samples were further diluted to 5 mg/mL in Dulbecco's PBS
435 (without Ca^{2+} and Mg^{2+}), and lipidomics analysis was performed as below.

436 ***Drug treatments and cell number quantification:*** RBL cells were treated with or without 20 μM DHA
437 in the presence or absence of betulin (inhibitor of SREBP processing) or GSK2194069 (FAS inhibitor).
438 Cells were treated for 72 h and then the cell number determined via fluorescein diacetate (FDA)
439 fluorescence. FDA is a cell viability probe which freely diffuses through cell membranes, but is trapped
440 in cells following de-acytelation by cytoplasmic esterases in viable cells. The number of viable cells is
441 then directly related to fluorescein fluorescence intensity. For the assay, cells were treated in 96-well
442 plates, gently washed with PBS, and then incubated with fluorescein diacetate (5 μg/mL in PBS) for 2
443 minutes at 37°C. The plates were then washed again to remove excess FDA and fluorescence was
444 measured at 488 nm excitation and 520 nm emission. For each experiment the number of cells per well
445 were normalized to untreated, unsupplemented cells.

446 ***Lipidomics:*** Detailed lipidomic analysis was performed by Lipotype, GmbH, as previously described[72].
447 Briefly, for preparation of crude cell membranes, cells were washed with phosphate buffered saline (PBS),
448 scraped in 10 mM Tris pH 7.4, and then homogenized with a 27-gauge needle. Nuclei were then pelleted
449 by centrifugation at 300 xg for 5 min. The supernatant was pelleted by centrifugation at 100,000 xg for 1
450 h at 4°C. The membrane pellet was then washed and resuspended in 150 mM ammonium bicarbonate.

451 *Lipids detected*: ceramide (Cer), Chol, SM, diacylglycerol (DAG), lactosyl ceramide (DiHexCer),
452 glucosyl/galactosyl ceramide (HexCer), sterol ester (SE), and triacylglycerol (TAG), as well as
453 phosphatidic acid (PA), phosphatidylcholine (PC), phosphatidylethanolamine (PE), phosphatidylglycerol
454 (PG), and phosphatidylinositol (PI), phosphatidylserine (PS), and their respective lysospecies (lysoPA,
455 lysoPC, lysoPE, lysoPI, and lysoPS) and ether derivatives (PC O-, PE O-, LPC O-, and LPE O-). Lipid

456 species were annotated according to their molecular composition as follows: [lipid class]-[sum of carbon
457 atoms in the FAs]:[sum of double bonds in the FAs];[sum of hydroxyl groups in the long chain base and
458 the FA moiety] (e.g., SM-32:2;1). When available, the individual FA composition according to the same
459 rule is given in brackets (e.g., 18:1;0-24:2;0)

460 *Lipid extraction*: Samples were extracted and analyzed as previously described (39,47), which is a
461 modification of a previously published method for shotgun lipidomics (48). Briefly, membrane samples
462 were suspended in 150 μL of 150 mM ammonium bicarbonate in water, spiked with 20 μL of internal
463 standard lipid mixture, and then extracted with 750 μL of a chloroform/methanol 10:1 (v/v) mixture for 2
464 h at 4_C with 1400 rpm shaking. After centrifugation (3 min, 3000 **g**) to facilitate phase partitioning, the
465 lower, lipid-containing, organic phase was collected (first-step extract), and the remaining water phase
466 was further extracted with 750 μL of a chloroform/methanol 2:1 (v/v) mixture under the same conditions.
467 Again the lower, organic phase was collected (second-step extract). Extracts were dried in a speed vacuum
468 concentrator, and 120 μL of a dried first-step extract underwent acetylation with 75 μL of an acetyl
469 chloride/chloroform 1:2 (v/v) mixture for 1 h to derivatize Chol. After the reaction was completed, the
470 mixture was dried. Then, 120 μL of a dried first-step extract and a derivatized extract were resuspended
471 in an acquisition mixture with 8 mM ammonium acetate (400 mM ammonium acetate in
472 methanol/chloroform/methanol/propan-2-ol, 1:7:14:28, v/v/v/v). Next, 120 μL of the second-step extract
473 was resuspended in an acquisition mixture with 30 μL 33% methylamine in methanol, in 60 mL
474 methanol/chloroform 1:5 (v/v). All liquid-handling steps were performed using a Hamilton (Reno, NV)
475 STARlet robotic platform with the Anti Droplet Control feature, ensuring the accuracy and reproducibility
476 of organic solvent pipetting.

477 *Lipid standards*: Synthetic lipid standards were purchased from Sigma-Aldrich (Chol D6), Larodan
478 (Solna, Sweden) Fine Chemicals (DAG and TAG), and Avanti Polar Lipids (all others). The standard lipid
479 mixtures were chloroform/ methanol 1:1 (v/v) solutions containing Cer 35:1;2, (D18:1;2, 17:0;0); Chol
480 D6; DAG 34:0;0 (17:0;0, 17:0;0); DiHexCer 30:1;2 (D18:1;2.12:0;0); HexCer 30:1;2 (D18:1;2.12:0;0);
481 LPA 17:0;0 (17:0;0); LPC 12:0;0 (12:0;0); LPE 17:1;0 (17:1;0); LPI 17:1;0 (17:1;0); LPS 17:1;0 (17:1;0);
482 PA 34:0;0 (17:0;0, 17:0;0); PC 34:0;0 (17:0;0, 17:0;0); PE 34:0;0 (17:0;0, 17:0;0); PG 34:0;0 (17:0;0,
483 17:0;0); PI 32:0;0 (16:0;0, 16:0;0); PS 34:0;0 (17:0;0, 17:0;0); SE 20:0;0 (20:0;0); SM 30:1;2 (18:1;2,
484 12:0;0); and TAG 51:0;0 (17:0;0, 17:0;0, 17:0;0).

485 *Lipid spectrum acquisition:* Extracts in the acquisition mixtures were infused with a robotic nanoflow ion
486 source (TriVersa NanoMate; Advion Biosciences, Ithaca, NY) into a mass spectrometer instrument (Q

487 Exactive, Thermo Scientific). Cer, DiHexCer, HexCer, lysolipids, and SM were monitored by negative
488 ion mode Fourier transform mass spectrometry (FT-MS). PA, PC, PE, PI, PS, and ether species were
489 monitored by negative ion mode FT tandem MS (FT-MS/MS). Acetylated Chol was monitored by positive
490 ion mode FTMS. SE, DAG, TAG, and species were monitored by positive ion mode FT-MS/MS.

491 *Lipid identification and quantification:* Automated processing of acquired mass spectra, and identification
492 and quantification of detected molecular lipid species were performed with the use of LipidXplorer
493 software (17). Only lipid identifications with a signal/noise ratio of >5, an absolute abundance of at least
494 1 pmol, and a signal intensity fivefold higher than in the corresponding blank samples were considered
495 for further data analysis.

496 ***C-laurdan spectroscopy:*** Membrane packing (related to order and fluidity) was determined via C-laurdan
497 spectroscopy as described [73,74]. Briefly, cells were washed with PBS and stained with 20 μg/mL C-laurdan
498 for 10 minutes on ice. The emission spectrum from isolated GPMVs was gathered from 400-550 nm with
499 excitation at 385 nm at 23°C. The GP was calculated according to the following equation:
500

501 $$GP = \frac{\sum_{420}^{460} I_x - \sum_{470}^{510} I_x}{\sum_{420}^{460} I_x + \sum_{470}^{510} I_x}$$

502

503 ***C-Laurdan spectral imaging:*** C-Laurdan imaging was performed as previously described [23,34,55,73,74].
504 Briefly, cells were washed with PBS and stained with 10 μg/mL C-Laurdan for 10 min on ice, then imaged
505 via confocal microscopy on a Nikon A1R with spectral imaging at 60x and excitation at 405 nm. The
506 emission was collected in two bands: 433–463 nm and 473–503 nm. MATLAB (MathWorks, Natick,
507 MA) was used to calculate the two-dimensional (2D) GP map, where GP for each pixel was calculated
508 from a ratio of the two fluorescence channels, as previously described [55]. Briefly, each image was binned
509 (2x2), background subtracted, and thresholded to keep only pixels with intensities greater than 3 standard
510 deviations of the background value in both channels. The GP image was calculated for each pixel using
511 the above equation. GP maps (pixels represented by GP value rather than intensity) were imported into
512 ImageJ. Line scans were drawn across individual cells. PM GP values were calculated as averages of the
513 peaks as values higher than 0.26. For internal membranes, average GP values were calculated from line
514 scans around the nucleus (visible as a dark spot in C-Laurdan images). At least 10 cells were imaged and
515 quantified per experiment with at least 4 individual experiments performed. Reported are the mean and
516 standard deviations of the average GP values for the individual experiments.

517

518 ***Amplex Red assay:*** Amplex Red cholesterol assay was performed (according to manufacturer
519 instructions; Invitrogen) to determine the abundance of cholesterol. Each reading was normalized to
520 protein concentration (determined by bicinchoninic acid (BCA) assay) in the same samples. Technical
521 triplicates were measured for each sample. Shown are values normalized to untreated cells. Reported are
522 the average and standard deviations from at least 3 independent biological replicates.

523

524 ***Western Blot:*** Cells were washed with ice cold PBS, then scraped into Laemmli lysis buffer (50mM Tris-
525 HCl, pH 8.0; 2% SDS; 5mM EDTA, pH8.0) supplemented with protease inhibitor cocktail. Protein
526 concentration was determined using BCA (Pierce), and equal amounts of protein were mixed with
527 reducing Laemmli sample buffer and loaded onto SDS-PAGE gels. Gels were transferred to PVDF
528 membranes, which were blocked in 5% BSA. Membranes were incubated with primary antibodies
529 overnight at 4°C, and detected with either AlexaFluor or HRP-tagged secondary antibodies. Membranes
530 were imaged using a BioRad ChemiDoc imager. The intensities of the bands were quantified normalized
531 to actin, and plotted as mean ± SD of $n \geq 3$ experiments.

532

533 ***Real Time Quantitative PCR:*** Total RNA was isolated via Trizol (Sigma) following the manufacturer's
534 protocol. Reverse transcriptase PCR was performed using the High Capacity cDNA Reverse Transcription
535 Kit from Applied Biosystems according to manufacturer's protocol. To quantify mRNA expression,
536 SYBR Fast MasterMix (2x) Universal Dye (#KK4602) from Kapa Biosystems was used in an Eppendorf
537 Realplex2 Mastercycler. Each primer set for each sample was run in triplicate with 1 ng of cDNA per
538 well. The primer sets used are:

539

Gene	**Forward Primer**	**Reverse Primer** 540
GAPDH	GTCTACTGGCGTCTTCACCA	GTGGCAGTGATGGCATGGAC
SCD1	GTGATGTTCCAGAGGAGGTACT	CAGGAACTCAGAAGCCCAGAA
SCD2	GGTGATGTTCCAGAGGAGGTATT	AACTGGAAGACCCCGAACTC

541

542 Expression changes were calculated using the delta delta C_T method. The data was standardized using a
543 previously published protocol [75] in which the average fold change was log transformed, mean centered,
544 and confidence intervals determined to evaluate statistical significance.

545

546 **Acknowledgements**

547 All confocal microscopy was performed at the Center for Advanced Microscopy, Department of
548 Integrative Biology and Pharmacology McGovern Medical School at the University of Texas Health
549 Science Center at Houston. We acknowledge funding from the Cancer Prevention Research Institute of
550 Texas (CPRIT; R1215), NIH/National Institute of General Medical Sciences (grant nos. GM114282,
551 GM124072, GM120351), and the Volkswagen Foundation (grant no. 93091).

552

553 **References**

554 1 Krogh, A., Larsson, B., von Heijne, G. & Sonnhammer, E. L. Predicting transmembrane protein topology
555 with a hidden Markov model: application to complete genomes. *Journal of molecular biology* **305**, 567-
556 580, (2001).
557 2 Janmey, P. A. & Kinnunen, P. K. Biophysical properties of lipids and dynamic membranes. *Trends in cell*
558 *biology* **16**, 538-546, (2006).
559 3 Los, D. A. & Murata, N. Membrane fluidity and its roles in the perception of environmental signals.
560 *Biochim Biophys Acta* **1666**, 142-157, (2004).
561 4 Andersen, O. S. & Koeppe, R. E., 2nd. Bilayer thickness and membrane protein function: an energetic
562 perspective. *Annu Rev Biophys Biomol Struct* **36**, 107-130, (2007).
563 5 Covino, R. *et al.* A eukaryotic sensor for membrane lipid saturation. *Molecular cell* **63**, 49-59, (2016).
564 6 daCosta, C. J., Dey, L., Therien, J. P. & Baenziger, J. E. A distinct mechanism for activating uncoupled
565 nicotinic acetylcholine receptors. *Nat Chem Biol* **9**, 701-707, (2013).
566 7 Marsh, D. Protein modulation of lipids, and vice-versa, in membranes. *Biochim Biophys Acta* **1778**, 1545-
567 1575, (2008).
568 8 Roux, A. *et al.* Membrane curvature controls dynamin polymerization. *Proc Natl Acad Sci U S A* **107**,
569 4141-4146, (2010).
570 9 Shi, Z. & Baumgart, T. Membrane tension and peripheral protein density mediate membrane shape
571 transitions. *Nature communications* **6**, 5974, (2015).
572 10 Rosholm, K. R. *et al.* Membrane curvature regulates ligand-specific membrane sorting of GPCRs in
573 living cells. *Nat Chem Biol* **13**, 724-729, (2017).
574 11 Sezgin, E., Levental, I., Mayor, S. & Eggeling, C. The mystery of membrane organization: composition,
575 regulation and roles of lipid rafts. *Nat Rev Mol Cell Biol* **18**, 361-374, (2017).
576 12 Lorent, J. H. *et al.* Structural determinants and functional consequences of protein affinity for membrane
577 rafts. *Nature communications* **8**, 1219, (2017).
578 13 Hazel, J. R. Thermal adaptation in biological membranes: is homeoviscous adaptation the explanation?
579 *Annu Rev Physiol* **57**, 19-42, (1995).
580 14 Sinensky, M. Homeoviscous adaptation--a homeostatic process that regulates the viscosity of membrane
581 lipids in Escherichia coli. *Proc Natl Acad Sci U S A* **71**, 522-525, (1974).
582 15 Ernst, R., Ejsing, C. S. & Antonny, B. Homeoviscous adaptation and the regulation of membrane lipids.
583 *Journal of molecular biology* **428**, 4776-4791, (2016).

16 Guschina, I. A. & Harwood, J. L. Mechanisms of temperature adaptation in poikilotherms. *FEBS Lett* **580**, 5477-5483, (2006).
17 Aguilar, P. S. *et al.* Molecular basis of thermosensing: a two-component signal transduction thermometer in Bacillus subtilis. *EMBO J* **20**, 1681-1691, (2001).
18 Halbleib, K. *et al.* Activation of the unfolded protein response by lipid bilayer stress. *Molecular cell* **67**, 673-684 e678, (2017).
19 Cao, J., Schwichtenberg, K. A., Hanson, N. Q. & Tsai, M. Y. Incorporation and clearance of omega-3 fatty acids in erythrocyte membranes and plasma phospholipids. *Clinical chemistry* **52**, 2265-2272, (2006).
20 Oliveira, T. V. *et al.* Impact of high cholesterol intake on tissue cholesterol content and lipid transfers to high-density lipoprotein. *Nutrition* **27**, 713-718, (2011).
21 Gerl, M. J. *et al.* Quantitative analysis of the lipidomes of the influenza virus envelope and MDCK cell apical membrane. *J Cell Biol* **196**, 213-221, (2012).
22 Sampaio, J. L. *et al.* Membrane lipidome of an epithelial cell line. *Proc Natl Acad Sci U S A* **108**, 1903-1907, (2011).
23 Levental, K. R. *et al.* Polyunsaturated lipids regulate membrane domain stability by tuning membrane order. *Biophys J* **110(8)**, 1800-1810, (2016).
24 Han, X. in *Lipidomics* 427-442 (John Wiley & Sons, Inc, 2016).
25 Klemm, R. W. *et al.* Segregation of sphingolipids and sterols during formation of secretory vesicles at the trans-Golgi network. *J Cell Biol* **185**, 601-612, (2009).
26 Ejsing, C. S. *et al.* Global analysis of the yeast lipidome by quantitative shotgun mass spectrometry. *Proc Natl Acad Sci U S A* **106**, 2136-2141, (2009).
27 Sinensky, M. Defective regulation of cholesterol biosynthesis and plasma membrane fluidity in a Chinese hamster ovary cell mutant. *Proc Natl Acad Sci U S A* **75**, 1247-1249, (1978).
28 Sinensky, M. Adaptive alteration in phospholipid composition of plasma membranes from a somatic cell mutant defective in the regulation of cholesterol biosynthesis. *J Cell Biol* **85**, 166-169, (1980).
29 Dymond, M. K. Mammalian phospholipid homeostasis: homeoviscous adaptation deconstructed by lipidomic data driven modelling. *Chem Phys Lipids* **191**, 136-146, (2015).
30 Dymond, M. K., Hague, C. V., Postle, A. D. & Attard, G. S. An in vivo ratio control mechanism for phospholipid homeostasis: evidence from lipidomic studies. *J R Soc Interface* **10**, 20120854, (2013).
31 Sodt, A. J., Venable, R. M., Lyman, E. & Pastor, R. W. Nonadditive Compositional Curvature Energetics of Lipid Bilayers. *Phys Rev Lett* **117**, 138104, (2016).
32 Almeida, P. F. Thermodynamics of lipid interactions in complex bilayers. *Biochim Biophys Acta* **1788**, 72-85, (2009).
33 Balogh, G. *et al.* Key role of lipids in heat stress management. *FEBS Lett* **587**, 1970-1980, (2013).
34 Levental, K. R. *et al.* omega-3 polyunsaturated fatty acids direct differentiation of the membrane phenotype in mesenchymal stem cells to potentiate osteogenesis. *Science advances* **3**, eaao1193, (2017).
35 Fan, Y. Y., McMurray, D. N., Ly, L. H. & Chapkin, R. S. Dietary (n-3) polyunsaturated fatty acids remodel mouse T-cell lipid rafts. *The Journal of nutrition* **133**, 1913-1920, (2003).
36 Stark, K. D. *et al.* Fatty acid compositions of serum phospholipids of postmenopausal women: a comparison between Greenland Inuit and Canadians before and after supplementation with fish oil. *Nutrition* **18**, 627-630, (2002).
37 Metcalf, R. G. *et al.* Effects of fish-oil supplementation on myocardial fatty acids in humans. *The American journal of clinical nutrition* **85**, 1222-1228, (2007).
38 van Blitterswijk, W. J., van der Meer, B. W. & Hilkmann, H. Quantitative contributions of cholesterol and the individual classes of phospholipids and their degree of fatty acyl (un)saturation to membrane fluidity measured by fluorescence polarization. *Biochemistry* **26**, 1746-1756, (1987).
39 Lande, M. B., Donovan, J. M. & Zeidel, M. L. The relationship between membrane fluidity and permeabilities to water, solutes, ammonia, and protons. *J Gen Physiol* **106**, 67-84, (1995).
40 Sessler, A. M., Kaur, N., Palta, J. P. & Ntambi, J. M. Regulation of stearoyl-CoA desaturase 1 mRNA stability by polyunsaturated fatty acids in 3T3-L1 adipocytes. *J Biol Chem* **271**, 29854-29858, (1996).
41 Levental, I. & Veatch, S. L. The continuing mystery of lipid rafts. *J. Mol. Biol.* **428**, 4749-4764, (2016).

42 Lin, X. *et al.* Domain stability in biomimetic membranes driven by lipid polyunsaturation. *J Phys Chem B* **120**, 11930-11941, (2016).
43 Yeagle, P. L. Cholesterol and the cell membrane. *Biochim Biophys Acta* **822**, 267-287, (1985).
44 Crockett, E. Cholesterol Function in Plasma Membranes from Ectotherms: Membrane-Specific Roles in Adaptation to Temperature. *Integrative and Comparative Biology* **38**, 298-304, (1998).
45 Raghow, R. *et al.* SREBPs: the crossroads of physiological and pathological lipid homeostasis. *Trends Endocrinol Metab* **19**, 65-73, (2008).
46 Sakai, J. *et al.* Molecular identification of the sterol-regulated luminal protease that cleaves SREBPs and controls lipid composition of animal cells. *Molecular cell* **2**, 505-514, (1998).
47 Tang, J. J. *et al.* Inhibition of SREBP by a small molecule, betulin, improves hyperlipidemia and insulin resistance and reduces atherosclerotic plaques. *Cell Metab* **13**, 44-56, (2011).
48 Kim, H. M. *et al.* A two-photon fluorescent probe for lipid raft imaging: C-laurdan. *Chembiochem* **8**, 553-559, (2007).
49 Owen, D. M. *et al.* Quantitative imaging of membrane lipid order in cells and organisms. *Nat Protoc* **7**, 24-35, (2011).
50 Kaiser, H. J. *et al.* Order of lipid phases in model and plasma membranes. *Proc Natl Acad Sci U S A* **106**, 16645-16650, (2009).
51 Gaus, K. *et al.* Condensation of the plasma membrane at the site of T lymphocyte activation. *J Cell Biol* **171**, 121-131, (2005).
52 Parasassi, T. *et al.* Quantitation of lipid phases in phospholipid vesicles by the generalized polarization of Laurdan fluorescence. *Biophys J* **60**, 179-189, (1991).
53 Sezgin, E. *et al.* Adaptive lipid packing and bioactivity in membrane domains. *PloS one* **10**, e0123930, (2015).
54 Levental, K. R. & Levental, I. Giant plasma membrane vesicles: models for understanding membrane organization. *Current topics in membranes* **75**, 25-57, (2015).
55 Sezgin, E., Waithe, D., Bernardino de la Serna, J. & Eggeling, C. Spectral imaging to measure heterogeneity in membrane lipid packing. *Chemphyschem* **16**, 1387-1394, (2015).
56 Feller, S. E., Gawrisch, K. & MacKerell, A. D., Jr. Polyunsaturated fatty acids in lipid bilayers: intrinsic and environmental contributions to their unique physical properties. *J Am Chem Soc* **124**, 318-326, (2002).
57 Briolay, A., Jaafar, R., Nemoz, G. & Bessueille, L. Myogenic differentiation and lipid-raft composition of L6 skeletal muscle cells are modulated by PUFAs. *Biochim Biophys Acta* **1828**, 602-613, (2013).
58 Seo, J. *et al.* Docosahexaenoic acid selectively inhibits plasma membrane targeting of lipidated proteins. *FASEB journal : official publication of the Federation of American Societies for Experimental Biology* **20**, 770-772, (2006).
59 Yaqoob, P. *et al.* Comparison of the effects of a range of dietary lipids upon serum and tissue lipid composition in the rat. *The international journal of biochemistry & cell biology* **27**, 297-310, (1995).
60 Kusakabe, T. *et al.* Fatty acid synthase is expressed mainly in adult hormone-sensitive cells or cells with high lipid metabolism and in proliferating fetal cells. *J Histochem Cytochem* **48**, 613-622, (2000).
61 Weiss, L. *et al.* Fatty-acid biosynthesis in man, a pathway of minor importance. Purification, optimal assay conditions, and organ distribution of fatty-acid synthase. *Biol Chem Hoppe Seyler* **367**, 905-912, (1986).
62 Murphy, E. J. Stable isotope methods for the in vivo measurement of lipogenesis and triglyceride metabolism. *J Anim Sci* **84 Suppl**, E94-104, (2006).
63 Nakagawa, Y., Sakumoto, N., Kaneko, Y. & Harashima, S. Mga2p is a putative sensor for low temperature and oxygen to induce OLE1 transcription in Saccharomyces cerevisiae. *Biochem Biophys Res Commun* **291**, 707-713, (2002).
64 Tiku, P. E. *et al.* Cold-induced expression of delta 9-desaturase in carp by transcriptional and posttranslational mechanisms. *Science* **271**, 815-818, (1996).
65 Burns, M. *et al.* Miscibility Transition Temperature Scales with Growth Temperature in a Zebrafish Cell Line. *Biophys J* **113**, 1212-1222, (2017).
66 Eberle, D. *et al.* SREBP transcription factors: master regulators of lipid homeostasis. *Biochimie* **86**, 839-848, (2004).

689 67 Yahagi, N. *et al.* A crucial role of sterol regulatory element-binding protein-1 in the regulation of
690 lipogenic gene expression by polyunsaturated fatty acids. *J Biol Chem* **274**, 35840-35844, (1999).
691 68 Hannah, V. C. *et al.* Unsaturated fatty acids down-regulate srebp isoforms 1a and 1c by two mechanisms
692 in HEK-293 cells. *J Biol Chem* **276**, 4365-4372, (2001).
693 69 Xu, J. *et al.* Polyunsaturated fatty acids suppress hepatic sterol regulatory element-binding protein-1
694 expression by accelerating transcript decay. *J Biol Chem* **276**, 9800-9807, (2001).
695 70 Radanovic, T. *et al.* An Emerging Group of Membrane Property Sensors Controls the Physical State of
696 Organellar Membranes to Maintain Their Identity. *BioEssays : news and reviews in molecular, cellular*
697 *and developmental biology*, e1700250, (2018).
698 71 Pirro, M. *et al.* Plasma free fatty acid levels and the risk of ischemic heart disease in men: prospective
699 results from the Quebec Cardiovascular Study. *Atherosclerosis* **160**, 377-384, (2002).
700 72 Tulodziecka, K. *et al.* Remodeling of the postsynaptic plasma membrane during neural development. *Mol*
701 *Biol Cell* **27**, 3480-3489, (2016).
702 73 Sezgin, E. *et al.* Elucidating membrane structure and protein behavior using giant plasma membrane
703 vesicles. *Nat Protoc* **7**, 1042-1051, (2012).
704 74 Levental, K. R. & Levental, I. Isolation of giant plasma membrane vesicles for evaluation of plasma
705 membrane structure and protein partitioning. *Methods in molecular biology* **1232**, 65-77, (2015).
706 75 Willems, E., Leyns, L. & Vandesompele, J. Standardization of real-time PCR gene expression data from
707 independent biological replicates. *Analytical biochemistry* **379**, 127-129, (2008).
708